

Reactivity of μ -Hydroxodizinc(II) Centers in Enzymatic Catalysis through Model Studies

Natalia V. Kaminskaia, Chuan He, and Stephen J. Lippard*

Department of Chemistry, Massachusetts Institute of Technology, Cambridge, Massachusetts 02139

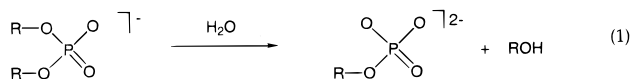
Received February 16, 2000

The stable dinuclear complex $[\text{Zn}_2(\text{BPAN})(\mu\text{-OH})(\mu\text{-O}_2\text{PPh}_2)](\text{ClO}_4)_2$, where BPAN = 2,7-bis[2-(2-pyridylethyl)-aminomethyl]-1,8-naphthyridine, was chosen as a model to investigate the reactivity of (μ -hydroxo)dizinc(II) centers in metallohydrolases. Two reactions, the hydrolysis of phosphodiester and the hydrolysis of β -lactams, were studied. These two processes are catalyzed *in vivo* by zinc(II)-containing enzymes: P1 nucleases and β -lactamases, respectively. The former catalyzes the hydrolysis of single-stranded DNA and RNA. β -Lactamases, expressed in many types of pathogenic bacteria, are responsible for the hydrolytic degradation of β -lactam antibiotic drugs. In the first step of phosphodiester hydrolysis promoted by the dinuclear model complex, the substrate replaces the bridging diphenylphosphinate. The bridging hydroxide serves as a general base to deprotonate water, which acts as a nucleophile in the ensuing hydrolysis. The dinuclear model complex is only 1.8 times more reactive in hydrolyzing phosphodiester than a mononuclear analogue, $\text{Zn}(\text{bpta})(\text{OTf})_2$, where bpta = *N,N*-bis-(2-pyridylmethyl)-*tert*-butylamine. Hydrolysis of nitrocefin, a β -lactam antibiotic analogue, catalyzed by $[\text{Zn}_2(\text{BPAN})(\mu\text{-OH})(\mu\text{-O}_2\text{PPh}_2)](\text{ClO}_4)_2$ involves monodentate coordination of the substrate via its carboxylate group, followed by nucleophilic attack of the zinc(II)-bound terminal hydroxide at the β -lactam carbonyl carbon atom. Collapse of the tetrahedral intermediate results in product formation. Mononuclear complexes $\text{Zn}(\text{cyclen})(\text{NO}_3)_2$ and $\text{Zn}(\text{bpta})(\text{NO}_3)_2$, where cyclen = 1,4,7,10-tetraazacyclododecane, are as reactive in the β -lactam hydrolysis as the dinuclear complex. Kinetic and mechanistic studies of the phosphodiester and β -lactam hydrolyses indicate that the bridging hydroxide in $[\text{Zn}_2(\text{BPAN})(\mu\text{-OH})(\mu\text{-O}_2\text{PPh}_2)](\text{ClO}_4)_2$ is not very reactive, despite its low $\text{p}K_{\text{a}}$ value. This low reactivity presumably arises from the two factors. First, the bridging hydroxide and coordinated substrate in $[\text{Zn}_2(\text{BPAN})(\mu\text{-OH})(\text{substrate})]^{2+}$ are not aligned properly to favor nucleophilic attack. Second, the nucleophilicity of the bridging hydroxide is diminished because it is simultaneously bound to the two zinc(II) ions.

Introduction

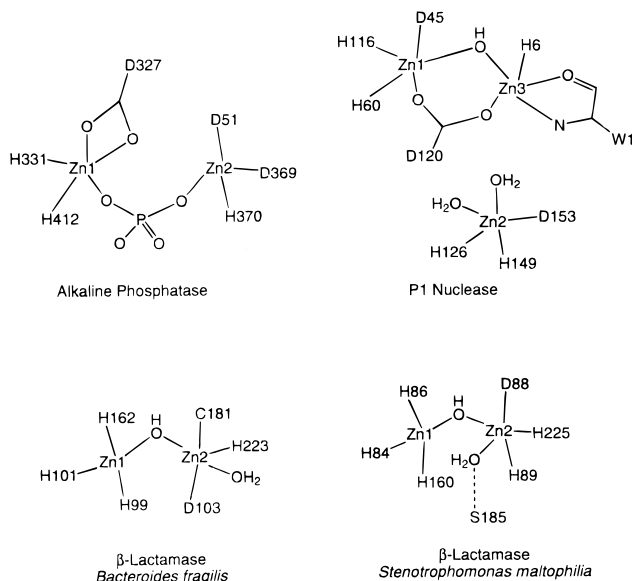
Metallohydrolases are hydrolytic enzymes that depend on metal ions, usually divalent zinc, cobalt, and manganese, for catalysis.¹ The mechanisms of enzymes containing a single metal ion, such as carboxypeptidase and carbonic anhydrase, have been extensively studied and are relatively well understood.² Dinuclear metallohydrolases have been studied to a lesser extent.¹ It is often proposed that a bridging hydroxide ion, which occurs in numerous dinuclear enzymes, serves as a nucleophile that attacks metal-bound substrates.^{2,3} The low $\text{p}K_{\text{a}}$ value for the bridging water at dinuclear sites results in a higher local concentration of hydroxide ion compared to that afforded at mononuclear centers. However, simultaneous coordination of hydroxide to two metal ions also results in tighter binding and lowered nucleophilicity. The enzymes Ser/Thr phosphatase, P1 nuclease, aminopeptidases, and class B β -lactamases are among Zn(II)-containing metallohydrolases that have two hydroxide-bridged zinc ions at the active sites.² Their respective mechanisms have been investigated but remain somewhat controversial. A recent spectroscopic study of aminopeptidase from *Aeromonas proteolytica* suggested a shift of the bridging hydroxide to a terminal position upon substrate binding. The terminal OH^- then attacks coordinated substrates.⁴

Phosphate ester hydrolysis (eq 1) *in vivo* is effected by a group of enzymes that are usually metal-dependent. This group



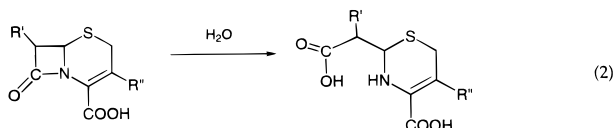
includes several zinc(II) enzymes, such as P1 nuclease and alkaline phosphatase, that have two zinc(II) ions at their active sites (Scheme 1). The former preferentially catalyzes the hydrolysis of single-stranded DNA and RNA, whereas the latter

Scheme 1

(1) Wilcox, D. E. *Chem. Rev.* **1996**, *96*, 2435–2458.(2) Lipscomb, W. N.; Sträter, N. *Chem. Rev.* **1996**, *96*, 2375–2433.(3) Wang, Z.; Fast, W.; Benkovic, S. J. *Biochemistry* **1999**, *38*, 10013–10023.(4) Bennett, B.; Holz, R. C. *J. Am. Chem. Soc.* **1997**, *119*, 1923–1933.

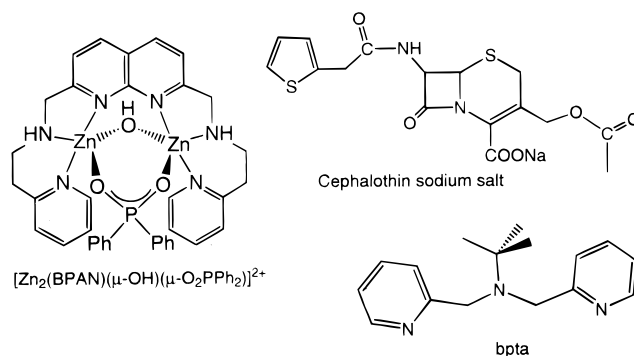
exhibits broad selectivity in phosphate monoester hydrolysis. The mechanisms of both reactions have been proposed to involve attack of the phosphorus atom by the bound hydroxide. It is not clear, however, whether the attacking hydroxide is in a terminal or bridging position. Notably, the X-ray structure of alkaline phosphatase does not show a bridging ligand between the two zinc(II) ions, whereas the structure of P1 nuclease reveals the presence of both the bridging and the terminal aqua ligands, either of which could act as the nucleophile precursor.^{2,5,6}

Hydrolysis of β -lactam antibiotics (eq 2) is a key reaction in bacterial drug resistance because it converts an active compound into one that is harmless to the organism.^{7,8} β -Lactamases,



enzymes that hydrolyze β -lactams, are expressed in numerous types of bacteria, many of which are pathogenic to humans.^{9–12} The periplasmic concentrations of β -lactamases are unusually high and can exceed 1 mM.¹³ These high concentrations, combined with the efficiency and broad specificity of β -lactamases, result in a loss of antibiotic effectiveness for the treatment of bacterial infections. Serine β -lactamases, containing a serine residue at the active site, are relatively well studied.¹³ On the basis of the mechanism of action deduced for these enzymes, clinically useful inhibitors have been synthesized and used with the respective antibiotic for treatment of the resistant infections. On the other hand, there has been much less mechanistic work on metallo- β -lactamases, which are zinc(II)-dependent enzymes that do not have clinically useful inhibitors.^{3,14} The crystal structures of three such metallo- β -lactamases have been reported^{15–17} and reveal dinuclear zinc(II) sites, coordinated predominantly by histidine ligands, as illustrated in Scheme 1. The *Bacillus cereus* metallo- β -lactamase was also crystallized with one zinc ion at the active site.¹⁸ By analogy with other metallohydrolases, such as carboxypeptidase, the catalytic mechanism was postulated to involve a metal-bound hydroxide that attacks the carbonyl carbon atom of the β -lactam ring.¹⁵ Present enzymatic data, however, are insufficient to deduce the mechanism by which metallo- β -lactamase operates. In particular, it is unknown whether hydrolysis occurs by direct nucleophilic attack or by general-base catalysis. The apparent need for two zinc ions at the active site remains to be elucidated.

Scheme 2



The complexity of enzymes often precludes a detailed assessment of their catalytic mechanisms. Simpler model compounds allow straightforward analysis of kinetic data and elucidation of the reaction mechanisms, establishing paradigms of reactivity that often can be transferred to the natural systems.^{19–25} We recently reported the synthesis and characterization of the dimetallic complex $[Zn_2(BPAN)(\mu-OH)(\mu-O_2PPh_2)](ClO_4)_2$ (Scheme 2), where BPAN = 2,7-bis[2-(2-pyridylethyl)aminomethyl]-1,8-naphthyridine. This complex efficiently catalyzes transesterification of 2-hydroxypropyl-*p*-nitrophenyl phosphate (HPNP); it is 6 times more reactive than the mononuclear complex $Zn(bpta)(OTf)_2$.²⁶ In the present study we take a more intensive look into the reactivity of this novel compound that functionally models dinuclear metallohydrolases. We report that the complex $[Zn_2(BPAN)(\mu-OH)(\mu-O_2PPh_2)](ClO_4)_2$ efficiently promotes the hydrolysis of phosphodiester and β -lactam substrates, mimicking the enzymes P1 nuclease and β -lactamase, respectively. The activity of this dinuclear complex is compared to that of the respective mononuclear complexes as well as dinuclear models of metallo- β -lactamase based on other dinucleating ligand systems recently discussed.²⁷

Experimental Section

Chemicals. The salts $Zn(NO_3)_2 \cdot 6H_2O$, zinc trifluoromethanesulfonate $Zn(OTf)_2$, $Zn(ClO_4)_2 \cdot 6H_2O$, and $NaClO_4$ were obtained from Aldrich. Reagents 2-(2-aminoethyl)pyridine, 2-amino-6-picoline, selenium dioxide, phosphorus oxychloride, ethyl acetate, and $NaBH_4$; hydrogenation catalyst 5% palladium on calcium carbonate; and the ligand cyclen were obtained from Aldrich. Succinic acid sodium salt hexahydrate and $LiOH \cdot H_2O$ were obtained from Fluka. The deuterium-containing compounds D_2O , $DMSO-d_6$, acetone- d_6 , chloroform- d_1 , and dichloromethane- d_2 were purchased from Cambridge Isotope Laboratories. Alanine, sodium salts of penicillin G, cephalothin, and the diester substrate nitrocefirin, 2-(2,4-dinitroethyl)-(6*R*,7*R*)-7-(2-thienylacetamide)-ceph-3-em-4-carboxylic acid, *E* isomer, was kindly donated by Merck. These and all other chemicals were of reagent grade.

CAUTION: Some of the syntheses and procedures described below involve compounds that contain the perchlorate ion, which can detonate

- (5) Kim, E. E.; Wyckoff, H. W. *J. Mol. Biol.* **1991**, *218*, 449–464.
- (6) Volbeda, A.; Lahm, A.; Sakiyama, F.; Suck, D. *EMBO J.* **1991**, *10*, 1607.
- (7) Frère, J.-M.; Dubus, A.; Galleni, M.; Matagne, A.; Amicosante, G. *Biochem. Soc. Trans.* **1999**, *27*, 58–63.
- (8) Cohen, M. L. *Science* **1992**, *257*, 1050–1055.
- (9) Rasmussen, B. A.; Bush, K. *Antimicrob. Agents Chemother.* **1997**, *41*, 223–232.
- (10) Livermore, D. M. *J. Antimicrob. Chemother. Suppl. D* **1998**, *41*, 25–41.
- (11) Bush, K. *Clin. Infect. Dis.* **1998**, *27*, S48–S53.
- (12) Rosdahl, V. T. *Dan. Med. Bull.* **1986**, *33*, 175–184.
- (13) Page, M. I.; Laws, A. P. *Chem. Commun.* **1998**, 1609–1617.
- (14) Wang, Z.; Fast, W.; Benkovic, S. J. *J. Am. Chem. Soc.* **1998**, *120*, 10788–10789.
- (15) Concha, N. O.; Rasmussen, B. A.; Bush, K.; Herzberg, O. *Structure* **1996**, *4*, 823–836.
- (16) Ullah, J. H.; Walsh, T. R.; Taylor, I. A.; Emery, D. C.; Verma, C. S.; Gamblin, S. J.; Spencer, J. *J. Mol. Biol.* **1998**, *284*, 125–136.
- (17) Fabiane, S. M.; Sohi, M. K.; Wan, T.; Payne, D. J.; Bateson, J. H.; Mitchell, T.; Sutton, B. J. *Biochemistry* **1998**, *37*, 12404–12411.
- (18) Carfi, A.; Pares, S.; Duée, E.; Galleni, M.; Duez, C.; Frère, J.M.; Dideberg, O. *EMBO J.* **1995**, *14*, 4914–4921.

- (19) Kimura, E.; Koike, T. *Adv. Inorg. Chem.* **1997**, *44*, 229–261.
- (20) Gultneh, Y.; Khan, A. R.; Blaise, D.; Chaudhry, S.; Ahvazi, B.; Marvey, B. B.; Butcher, R. J. *J. Inorg. Biochem.* **1999**, *75*, 7–18.
- (21) Jurek, P.; Martell, A. E. *Inorg. Chim. Acta* **1999**, *287*, 47–51.
- (22) Molenveld, P.; Stikvoort, W. M. G.; Kooijman, H.; Spek, A. L.; Engbersen, J. F. J.; Reinhoudt, D. N. *J. Org. Chem.* **1999**, *64*, 3896–3906.
- (23) Itoh, T.; Hisada, H.; Usui, Y.; Fujii, Y. *Inorg. Chim. Acta* **1998**, *283*, 51–60.
- (24) Kamitani, J.; Kawahara, R.; Yashiro, M.; Komiyama, M. *Chem. Lett.* **1998**, 1047–1048.
- (25) Schneider, H.-J.; Rammo, J.; Hettich, R. *Angew. Chem., Int. Ed. Engl.* **1993**, *32*, 1716–1719.
- (26) He, C.; Lippard, S. J. *J. Am. Chem. Soc.* **2000**, *122*, 184–185.
- (27) Kaminskaia, N. V.; Spingler, B.; Lippard, S. J. *J. Am. Chem. Soc.* **2000**, in press.

explosively and without warning. Although we have not encountered any problems with the reported compounds, all due precautions should be taken.

Physical Measurements. UV-vis spectrophotometric experiments were performed on a Cary 1E instrument equipped with temperature control. The temperature was monitored directly inside the spectrophotometric cell with a thermocouple. Solution IR spectra were recorded on a Biorad FTS-135 FTIR spectrometer between 1000 and 3500 cm^{-1} using a CaF_2 cell. The ambient temperature was measured before and after each experiment and the average reading is reported. Proton and carbon-13 NMR spectra were recorded at 500 and 125 MHz, respectively, on Varian 500 and 501 NMR spectrometers. Phosphorus-31 spectra were recorded on a Varian Mercury-300 instrument at 121.4 MHz. The external reference was 85% H_3PO_4 with a chemical shift set at 0.00 ppm. All of the NMR instruments were equipped with temperature controllers.

Ligand Syntheses. Synthesis reactions were carried out under either N_2 or Ar atmospheres. The precursor to BPAN, 2,7-dimethyl-1,8-naphthyridine, was synthesized from 6-methyl-2-pyridinamine and ethyl acetoacetate in four steps as described previously.²⁸ 2,7-Dimethyl-1,8-naphthyridine was converted to 1,8-naphthyridine-2,7-dicarboxaldehyde by a modification of the published procedure,^{26,28} as described in the Supporting Information. Condensation of 1,8-naphthyridine-2,7-dicarboxaldehyde and 2-(2-aminoethyl)pyridine, followed by reduction with NaBH_4 gave BPAN as the final product.²⁶ The yield was 1.26 g (80%). ^1H NMR in a 1:1 mixture of $\text{DMSO}-d_6$ and D_2O : δ 8.25 m (4H), 7.60 t ($J = 8$ Hz, 2H), 7.45 d ($J = 9$ Hz, 2H), 7.20 d ($J = 8$ Hz, 2H), 7.10 t ($J = 5$ Hz, 2H), 3.95 s (4H), 2.90 m (8H). These chemical shifts differ from those in CDCl_3 .²⁶ The ligand *N,N*-bis(2-pyridylmethyl)-*tert*-butylamine (bpta) was synthesized as described previously.²⁹

Complex Syntheses. The complex $[\text{Zn}_2(\text{BPAN})(\mu\text{-OH})(\mu\text{-O}_2\text{PPh}_2)](\text{ClO}_4)_2$ was prepared from BPAN, $\text{Zn}(\text{OTf})_2$, LiO_2PPh_2 , and NaClO_4 in aqueous ethanol according to the published procedure.²⁶ The yield was 0.030 g (30%). ^1H NMR in a 1:1 mixture of $\text{DMSO}-d_6$ and D_2O : δ 8.30 br (2H), 7.60 br (4H), 7.20 br (6H), 4.38 br (2H), 3.40 br (2H), 3.0 m (8H). The mononuclear complexes $\text{Zn}(\text{cyclen})(\text{NO}_3)_2$, $\text{Zn}(\text{bpta})(\text{OTf})_2$, and $\text{Zn}(\text{bpta})(\text{NO}_3)_2$ were prepared in situ by mixing equivalent amounts of the corresponding ligand and zinc(II) salt.²⁶

Stability of $[\text{Zn}_2(\text{BPAN})(\mu\text{-OH})(\mu\text{-O}_2\text{PPh}_2)](\text{ClO}_4)_2$ in Water. The composition of the complex in aqueous solution was studied by ^1H NMR titration experiments at 293 K. The solvent was a 1:1 mixture of D_2O and $\text{DMSO}-d_6$. The initial concentration of the ligand BPAN was determined by calibration with Ala as an internal standard and was found to be 0.0380 M. In the titration experiments, two solutions that contained aliquots of $\text{Zn}(\text{ClO}_4)_2 \cdot 6\text{H}_2\text{O}$ and LiO_2PPh_2 , respectively, were added in a stepwise manner to the NMR tube that contained a solution of BPAN. The two titrating solutions were 1.00 M in $\text{Zn}(\text{ClO}_4)_2 \cdot 6\text{H}_2\text{O}$ and 1.00 M in LiO_2PPh_2 , prepared from $\text{LiOH} \cdot \text{H}_2\text{O}$ and $\text{Ph}_2\text{PO}_2\text{H}$, respectively. Each was dissolved in a 1:1 mixture of D_2O and $\text{DMSO}-d_6$. After every addition of the two titrating solutions a ^1H NMR spectrum was taken. The concentrations of the free ligand and the complex were determined from the respective integral areas with an estimated error of 5–10%.

The equilibrium constant for the binding of two zinc(II) ions to BPAN was estimated on the basis of ^1H NMR titration measurements. A solution containing 0.0380 M each of BPAN and LiO_2PPh_2 , and 0.076 M of $\text{Zn}(\text{ClO}_4)_2 \cdot 6\text{H}_2\text{O}$, in a 1:1 mixture of D_2O and $\text{DMSO}-d_6$, was diluted 10–70-fold. The number and positions of the peaks in the ^1H NMR spectra of the diluted solutions remained unchanged. On the basis of ^1H NMR sensitivity (>5%), the concentration of free ligand would be $<2.5 \times 10^{-5}$ M if $[\text{BPAN}]_T$ was 5×10^{-4} M. Therefore, the value for the overall binding constant is $>1.0 \times 10^{10} \text{ M}^{-2}$.

Kinetics of Phosphate Diester Hydrolysis. The solvent was a 4:1 mixture of 0.05 M HEPES buffer in H_2O and acetonitrile, and the temperature was 313 K. The reported pH values of the solutions correspond to the aqueous component. The stock solutions of the

complexes and substrate bis(*p*-nitrophenyl)phosphate were 0.020 and 0.010 M, respectively. The initial concentrations of the reactants in the reaction mixture were varied and are specified in the respective table footnotes and figure captions. In a typical kinetic experiment, all reagents were mixed in a spectrophotometric cell and allowed to equilibrate for 10 min inside the temperature-controlled unit before data collection began. The hydrolysis reaction was followed by monitoring the growth in absorbance of the product, *p*-nitrophenolate, at 400 nm. The reactions were followed only for the first 1% of hydrolysis to avoid significant changes in the initial concentrations of the reactants. The observed rate constants were determined from the initial rates and the initial concentration of bis(*p*-nitrophenyl)phosphate. The effect of the water concentration on hydrolysis was studied in 10% and 20% aqueous acetonitrile solutions at 313 K. The observed rate constant for the hydrolysis promoted by the dinuclear complex in 98% acetonitrile was estimated to be lower than $2.3 \times 10^{-11} \text{ s}^{-1}$ at 313 K on the basis of UV-vis experiments. This value is almost identical to that of background hydrolysis. Therefore, low solubility of the reactants in pure water and very slow hydrolysis at higher acetonitrile levels in aqueous solution limited the experimentally attainable range of possible water concentrations.

Binding of Cephalothin to $[\text{Zn}_2(\text{BPAN})(\mu\text{-OH})(\mu\text{-O}_2\text{PPh}_2)](\text{ClO}_4)_2$. (a) **Carbon-13 NMR Experiments.** The solution was initially 0.150 M in complex and 0.150 M in the sodium salt of cephalothin. The solvent was neat $\text{DMSO}-d_6$, and the temperature was 293 K. ^{13}C NMR (ppm) in $\text{DMSO}-d_6$ for the sodium salt of cephalothin (carbonyl region): δ 170.6 (C(O) ester), 170.0 (C(O) amide), 164.3 (COO), 163.1 (C(O) lactam). ^{13}C NMR (ppm) in $\text{DMSO}-d_6$ for cephalothin in the presence of $[\text{Zn}_2(\text{BPAN})(\mu\text{-OH})(\mu\text{-O}_2\text{PPh}_2)](\text{ClO}_4)_2$ (carbonyl region): δ 170.4 br (C(O) ester and C(O) amide), 165.9 (COO), 164.2 (C(O) lactam).

(b) **Solution IR Experiments.** The initial concentrations of $[\text{Zn}_2(\text{BPAN})(\mu\text{-OH})(\mu\text{-O}_2\text{PPh}_2)](\text{ClO}_4)_2$ and cephalothin were 0.050 M each, and the solvent was pure DMSO. The temperature was 293 ± 0.5 K. IR (cm^{-1}) for the sodium salt of cephalothin in DMSO (carbonyl region): 1773 ($\nu_{\text{C=O}}^{\beta\text{-lactam}}$), 1731 ($\nu_{\text{C=O}}^{\text{ester}}$), 1680 ($\nu_{\text{C=O}}^{\text{amide}}$), 1617 (asym ν_{COO}). IR (cm^{-1}) for cephalothin in the presence of $[\text{Zn}_2(\text{BPAN})(\mu\text{-OH})(\mu\text{-O}_2\text{PPh}_2)](\text{ClO}_4)_2$ in DMSO (carbonyl region): 1772 ($\nu_{\text{C=O}}^{\beta\text{-lactam}}$), 1736 ($\nu_{\text{C=O}}^{\text{ester}}$), 1682 ($\nu_{\text{C=O}}^{\text{amide}}$), 1626 (asym ν_{COO}).

Displacement of Diphenylphosphinate in $[\text{Zn}_2(\text{BPAN})(\mu\text{-OH})(\mu\text{-O}_2\text{PPh}_2)](\text{ClO}_4)_2$ by β -Lactam Substrates. This reaction was followed by using ^{31}P NMR spectroscopy. The solvent was either a 9:1 mixture or a 1:1 mixture of D_2O and $\text{DMSO}-d_6$, and the temperature was 293 K. In a typical experiment the concentrations of $[\text{Zn}_2(\text{BPAN})(\mu\text{-OH})(\mu\text{-O}_2\text{PPh}_2)](\text{ClO}_4)_2$ and the sodium salt of penicillin G were 5.00×10^{-3} M and 2.50×10^{-2} M, respectively. In control experiments the concentration of LiO_2PPh_2 was 0.300 M. Usually, up to 300 scans were taken to obtain a satisfactory signal-to-noise ratio.

Kinetics of β -Lactam Hydrolysis. The kinetic experiments were performed on a UV-vis spectrophotometer. The solvent was either a 9:1 mixture of 0.050 M HEPES buffer (in H_2O) and DMSO or a 9:1 mixture of acetone and DMSO. The reported pH values of the solutions correspond to the aqueous component. The temperature was 313 K unless stated otherwise. The extinction coefficients of the substrate, nitrocefin, and its hydrolysis product were determined previously.²⁷ Stock solutions of complexes, nitrocefin, and inhibitors (sodium succinate and sodium acetate) were freshly prepared in DMSO to avoid possible decomposition. The concentrations of the stock solutions of the complexes and nitrocefin were 0.010 M each. The exact concentration of nitrocefin in each experiment was determined from the absorbance at 390 nm and extinction coefficient ($\epsilon_{390} = 21\,000 \text{ M}^{-1} \text{ cm}^{-1}$). The concentrations of the stock solutions of inhibitors were varied and are specified in the respective figure captions. Typically, in each kinetic experiment all of the chemicals were mixed in a spectrophotometric cell and allowed to equilibrate for 2 min inside the temperature-controlled UV-vis spectrophotometer before starting data acquisition. With the exception of the catalytic experiment described in the Supporting Information, the data were recorded at 390 nm, the wavelength that corresponds to the maximum absorbance of nitrocefin. Because the product of the reaction also absorbs at 390 nm, the

(28) Chandler, C. J.; Deady, L. W.; Reiss, J. A.; Tzimos, V. *J. Heterocycl. Chem.* **1982**, *19*, 1017–1019.

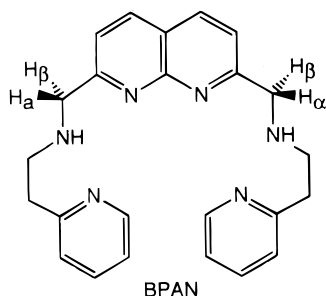
(29) Mok, H. J.; Davis, J. A.; Pal, S.; Mandal, S. K.; Armstrong, W. H. *Inorg. Chim. Acta* **1997**, *263*, 385–394.

extinction coefficient of nitrocefin was corrected to $13\,415\text{ M}^{-1}\text{ cm}^{-1}$, as described previously, to account for the product absorbance.²⁷ Usually the reaction was followed to only 3–5% conversion to avoid significant changes in the concentrations of the starting materials. The observed rate constants were then determined from the initial rates, the known concentrations of the substrates, and the corrected extinction coefficient of nitrocefin at 390 nm. The hydrolysis reactions in the absence of water were studied in neat DMSO and in a 1:9 mixture of DMSO and acetone as the solvents at 313 K. The solutions were dried over activated molecular sieves (4 Å) to remove any adventitious water prior to the addition of nitrocefin. The initial concentrations of the complex and nitrocefin were 5.0×10^{-4} and 3.8×10^{-5} M, respectively. The hydrolysis products of penicillin and nitrocefin in the presence of β -lactamases and zinc(II) complexes have been previously identified by spectroscopic methods.^{27,30–34} The ¹H NMR data for the hydrolysis product of cephalothin (Supporting Information) are very similar to those for hydrolyzed nitrocefin. All recorded ¹H NMR spectra are consistent with hydrolysis of the β -lactam ring being the sole reaction in the presence of $[\text{Zn}_2(\text{BPAN})(\mu\text{-OH})(\mu\text{-O}_2\text{PPh}_2)](\text{ClO}_4)_2$. Hydrolysis of the amide group and rearrangements were not observed.

Results and Discussion

The Structure of $[\text{Zn}_2(\text{BPAN})(\mu\text{-OH})(\mu\text{-O}_2\text{PPh}_2)](\text{ClO}_4)_2$ in Solution. The solid-state structure of $[\text{Zn}_2(\text{BPAN})(\mu\text{-OH})(\mu\text{-O}_2\text{PPh}_2)](\text{ClO}_4)_2$ (Scheme 2) reveals a symmetric dinuclear complex.²⁶ The two zinc(II) ions are bridged by the two exogenous ligands, hydroxide and diphenylphosphinate. The latter acts as a substrate analogue. In the solid state this complex satisfies all of the important requirements for a compound that mimics the active sites in Scheme 1. Conversion of dinuclear to mononuclear complexes in solution in the presence of water is known, however.³⁵ We therefore undertook a titration study to determine the integrity of this complex in aqueous solution.

The proton resonances of the two methylene groups in BPAN appear as a singlet at 3.95 ppm in the free ligand. Upon zinc(II) binding, the α and β protons in each methylene group become inequivalent and their respective resonances shift. They occur at 4.38 and 3.40 ppm in the ¹H NMR spectrum of $[\text{Zn}_2(\text{BPAN})(\mu\text{-OH})(\mu\text{-O}_2\text{PPh}_2)](\text{ClO}_4)_2$ in aqueous DMSO. Ti-



tration experiments were performed as described in the Experimental Section.

The concentrations of free and bound BPAN after each addition of Zn(II) salt were determined by integrating their respective resonances. The experimental titration curve is

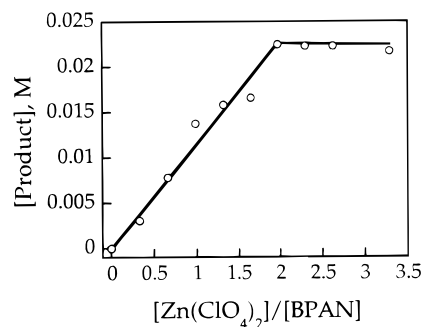


Figure 1. ¹H NMR titration of BPAN with $\text{Zn}(\text{ClO}_4)_2 \cdot 6\text{H}_2\text{O}$ and LiO_2PPh_2 .

depicted in Figure 1. The concentration of the complex increases as more Zn(II) salt and diphenylphosphinate are added to the reaction mixture containing BPAN. Notably, the concentration of the complex undergoes no further change once the $[\text{Zn}(\text{ClO}_4)_2]/[\text{ligand}]$ ratio reaches a value of two. This finding indicates that the complex exists as a stable dimetallic species in the presence of water. Dilution does not affect the ¹H NMR spectrum of $[\text{Zn}_2(\text{BPAN})(\mu\text{-OH})(\mu\text{-O}_2\text{PPh}_2)](\text{ClO}_4)_2$ (Experimental Section). These results indicate that $[\text{Zn}_2(\text{BPAN})(\mu\text{-OH})(\mu\text{-O}_2\text{PPh}_2)]^{2+}$ is the major species in solution under the reaction conditions.^{22,26,36}

The $\text{p}K_a$ value for deprotonation of the bridging water in $[\text{Zn}_2(\text{BPAN})(\mu\text{-OH}_2)(\mu\text{-O}_2\text{PPh}_2)](\text{ClO}_4)_3$ is 6.95 ± 0.05 , which compares well with those of an aqua ligand at the mononuclear zinc(II) site in carboxypeptidase and at the dinuclear site in aminopeptidases.^{26,37,38} The $\text{p}K_a$ value of the aqua ligand in the model complex (6.95) is higher than it is in purple acid phosphatase (4.7) because, in the latter, water is coordinated to a more acidic Fe^{3+} ion.³⁹ Zinc(II)-bound hydroxide forms at physiological pH in concentrations sufficiently high for efficient hydrolytic reaction chemistry. A second observed $\text{p}K_a$ of 8.7 for $[\text{Zn}_2(\text{BPAN})(\mu\text{-OH}_2)(\mu\text{-O}_2\text{PPh}_2)](\text{ClO}_4)_3$ was tentatively assigned to deprotonation of a terminally bound water that replaces diphenylphosphinate in $[\text{Zn}_2(\text{BPAN})(\mu\text{-OH})(\mu\text{-O}_2\text{PPh}_2)](\text{ClO}_4)_2$.^{22,26}

Phosphodiester Hydrolysis Promoted by $[\text{Zn}_2(\text{BPAN})(\mu\text{-OH})(\mu\text{-O}_2\text{PPh}_2)](\text{ClO}_4)_2$. Because phosphate esters are very stable toward hydrolysis, activated bis(*p*-nitrophenyl)phosphate was chosen as the substrate. In addition to its reactivity, hydrolysis of bis(*p*-nitrophenyl)phosphate affords *p*-nitrophenol, the conjugate base of which, *p*-nitrophenolate, absorbs intensely in the visible region. Hence, the kinetics could be conveniently followed.

The complex $[\text{Zn}_2(\text{BPAN})(\mu\text{-OH})(\mu\text{-O}_2\text{PPh}_2)](\text{ClO}_4)_2$ effects the hydrolysis of bis(*p*-nitrophenyl)phosphate to *p*-nitrophenol and *p*-nitrophenyl phosphate (eq S1 in Supporting Information). Further hydrolysis of *p*-nitrophenyl phosphate (eq S2) was not detected in the kinetic experiments because only the initial 1% of bis(*p*-nitrophenyl)phosphate hydrolysis was followed. Rate enhancements in reactions promoted by the dinuclear zinc complex are 1.8 and 9.2×10^3 relative to hydrolyses in the presence of Zn(bpta)(OTf)₂ or no zinc complex, respectively (Table 1).^{40,41} Control experiments indicate no inhibition of the hydrolysis rate by diphenylphosphinate if the substrate is present in excess.

(30) Murphy, B. P.; Pratt, R. F. *Biochem. J.* **1989**, *258*, 765–768.

(31) Laraki, N.; Franceschini, N.; Rossolini, G. M.; Santucci, P.; Meunier, C.; Pauw, E.; Amicosante, G.; Frère, J. M.; Galleni, M. *Antimicrob. Agents Chemother.* **1999**, *43*, 902–906.

(32) Koike, T.; Takamura, M.; Kimura, E. *J. Am. Chem. Soc.* **1994**, *116*, 8443–8449.

(33) Yang, Y.; Rasmussen, B. A.; Bush, K. *Antimicrob. Agents Chemother.* **1992**, *36*, 1155–1157.

(34) Felici, A.; Amicosante, G.; Oratore, A.; Strom, R.; Ledent, P.; Joris, B.; Fanuel, L.; Frère, J.-M. *Biochem. J.* **1993**, *291*, 151–155.

(35) He, C.; Lippard, S. J. *J. Am. Chem. Soc.* **1998**, *120*, 105–113.

(36) Chu, F.; Smith, J.; Lynch, V. M.; Anslyn, E. V. *Inorg. Chem.* **1995**, *34*, 5689–5690.

(37) Harris, M. N.; Ming, L.-J. *FEBS Lett.* **1999**, *455*, 321–324.

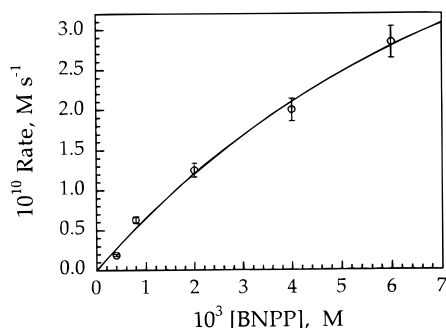
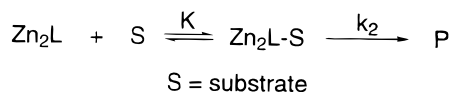
(38) Chen, G.; Edwards, T.; D'souza, V. M.; Holz, R. C. *Biochemistry* **1997**, *36*, 4278–4286.

(39) Durmus, A.; Eicken, C.; Sift, B. H.; Kratel, A.; Kappl, R.; Huttermann, J.; Krebs, B. *Eur. J. Biochem.* **1999**, *260*, 709–716.

Table 1. Observed Rate Constants (k_{obs}) for Hydrolysis of Bis(*p*-nitrophenyl)phosphate and Nitrocefin Promoted by Zinc(II) Complexes

Zn(II) complex	k_{obs} (s^{-1}) for bis(<i>p</i> -nitrophenyl)-phosphate ^a	k_{obs} (min^{-1}) for nitrocefin ^b
none	7.1×10^{-11} ^c	6.4×10^{-7}
Zn(NO ₃) ₂		$(0.8 \pm 0.2) \times 10^{-3}$
Zn(bpta)X ₂	$(3.7 \pm 0.4) \times 10^{-7}$ ^d	$(3.8 \pm 0.2) \times 10^{-3}$ ^e
Zn(cyclen)(NO ₃) ₂		$(1.7 \pm 0.2) \times 10^{-3}$
[Zn ₂ (BPAN)(μ -OH)-(μ -O ₂ PPh ₂)](ClO ₄) ₂	$(6.5 \pm 0.7) \times 10^{-7}$	$(1.8 \pm 0.3) \times 10^{-3}$

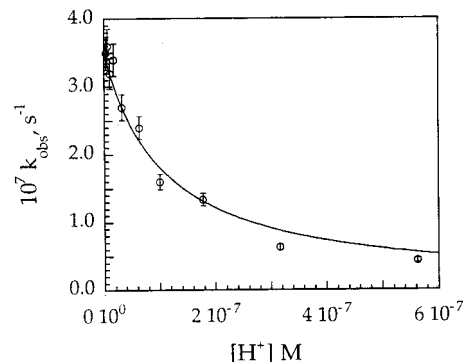
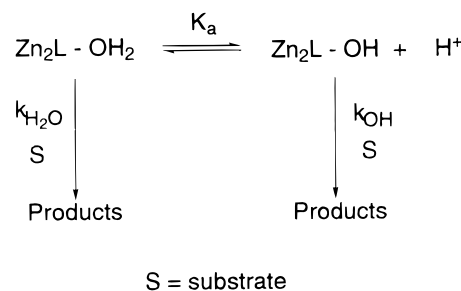
^a The initial concentration of bis(*p*-nitrophenyl)phosphate was 2.0×10^{-3} M; the initial concentrations of [Zn₂(BPAN)(μ -OH)(μ -O₂PPh₂)](ClO₄)₂ and mononuclear zinc(II) species were each 2.0×10^{-4} M. The solvent was a 4:1 mixture of 0.05 M HEPES buffer (pH 7.00) and acetonitrile, and the temperature was 313 K. ^b The initial concentration of nitrocefin was 3.8×10^{-5} M; the initial concentrations of [Zn₂(BPAN)(μ -OH)(μ -O₂PPh₂)](ClO₄)₂ and mononuclear zinc(II) complexes were each 5.0×10^{-4} M. The solvent was a 9:1 mixture of 0.05 M HEPES buffer (pH 6.95) and DMSO, and the temperature was 313 K. ^c References 25 and 26; extrapolated from rate measurements at 373 K, $\Delta S^\ddagger = 25.5$ eu. ^d X = OTf. ^e X = NO₃.

**Figure 2.** Effect of bis(*p*-nitrophenyl)phosphate concentration on the initial rate of its hydrolysis promoted by [Zn₂(BPAN)(μ -OH)(μ -O₂PPh₂)](ClO₄)₂. The initial concentration of the complex was 2.0×10^{-4} M.**Scheme 3**

The hydrolysis reaction is first order in bis(*p*-nitrophenyl)phosphate if it is present at a relatively low concentration, as the data in Figure 2 indicate. Diminution of the rate at higher concentrations reflects substrate coordination prior to hydrolysis, as illustrated in Scheme 3. When the experimental data were fit to eq 3, derived for the mechanism in Scheme 3, values for

$$v_o = \frac{Kk_2[\text{Zn}_2\text{L}][\text{S}]}{K[\text{S}] + 1} \quad (3)$$

the binding constant K and the microscopic rate constant k_2 of $86 \pm 32 \text{ M}^{-1}$ and $(4.1 \pm 1.2) \times 10^{-6} \text{ s}^{-1}$, respectively, were obtained. Evidently, bis(*p*-nitrophenyl)phosphate is a relatively weak ligand. Presumably, it displaces the substrate analogue diphenylphosphinate in [Zn₂(BPAN)(μ -OH)(μ -O₂PPh₂)](ClO₄)₂ and bridges the two zinc(II) ions. In a related study with a dicopper(II) calix[4]arene complex the respective binding constant for this substrate was 250 M^{-1} .⁴² Studies of 2-hydroxy-

**Figure 3.** Effect of the solution pH on bis(*p*-nitrophenyl)phosphate hydrolysis promoted by [Zn₂(BPAN)(μ -OH)(μ -O₂PPh₂)](ClO₄)₂. The initial concentrations of the complex and substrate were 2.0×10^{-4} and 2.0×10^{-3} M, respectively.**Scheme 4**

propyl-*p*-nitrophenyl phosphate (HPNP) transesterification by various dizinc(II) complexes yielded similar values.²²

Effects of pH on the Hydrolysis of Bis(*p*-nitrophenyl)phosphate. Raising the solution pH values resulted in more rapid hydrolysis, as the data in Figure 3 illustrate, presumably because the concentration of the more reactive species Zn₂L-OH is elevated at high pH. The experimental data were fit to eq 4, derived for the mechanism in Scheme 4. The best fit was

$$k_{\text{obs}} = \frac{k_{\text{H}_2\text{O}}[\text{H}^+] + k_{\text{OH}}K_a}{K_a + [\text{H}^+]} [\text{S}] \quad (4)$$

obtained when $k_{\text{H}_2\text{O}}$ was set to zero. This fit yielded the $\text{p}K_a$ value of 7.06 ± 0.05 , corresponding to the formation of the more reactive species. This kinetically determined $\text{p}K_a$ value is in excellent agreement with that for the bridging hydroxide in [Zn₂(BPAN)(μ -OH)(μ -O₂PPh₂)](ClO₄)₂ obtained in the potentiometric titration experiments.²⁶ Therefore, the bridging hydroxide acts as the reactive species, either a nucleophile or a general base, in the phosphate diester hydrolysis.

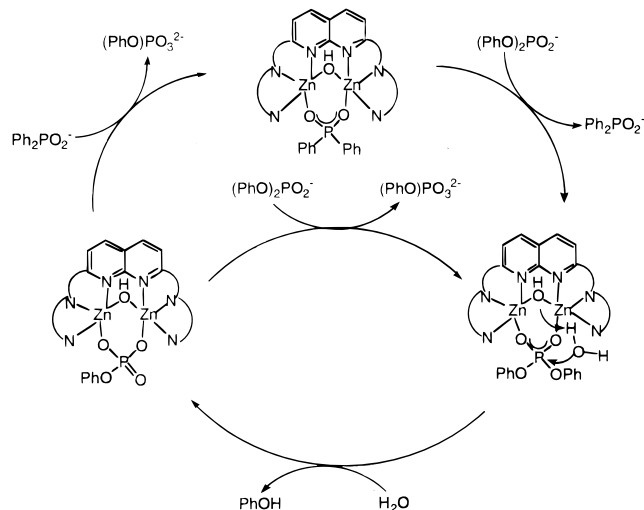
The exact role of the bridging hydroxide could be deduced from the effects of varying the water concentration on hydrolysis. If the bridging hydroxide serves as a nucleophile, the microscopic rate constant for hydrolysis of the bound substrate will be independent of water concentration. In the case of general-base catalysis by the bridging hydroxide, hydrolysis should depend on water concentration. When [Zn₂(BPAN)(μ -OH)(μ -O₂PPh₂)](ClO₄)₂ and bis(*p*-nitrophenyl)phosphate were allowed to react in DMSO and acetonitrile as the solvents in the presence of 0.12 M H₂O, no hydrolysis was detected for 20 h at 313 K. Longer incubation times resulted in decomposition of the complex and were therefore not pursued. The k_{obs} values for hydrolysis in 10% and 20% aqueous acetonitrile solutions

(40) Kirby, A. J.; Younas, M. *J. Chem. Soc. B* **1970**, 510–513.(41) Chung, Y.; Akkaya, E. U.; Venkatachalam, T. K.; Gzarnik, A. W. *Tetrahedron Lett.* **1990**, 31, 5413–5416.(42) Molenveld, P.; Engbersen, J. F. J.; Kooijman, H.; Spek, A. L.; Reinhoudt, D. N. *J. Am. Chem. Soc.* **1998**, 120, 6726–6737.

are $(1.08 \pm 0.15) \times 10^{-6}$ and $(0.65 \pm 0.15) \times 10^{-6} \text{ s}^{-1}$, respectively. Clearly, decreasing the concentration of water slows the hydrolysis rate. This finding suggests a general-base mechanism.

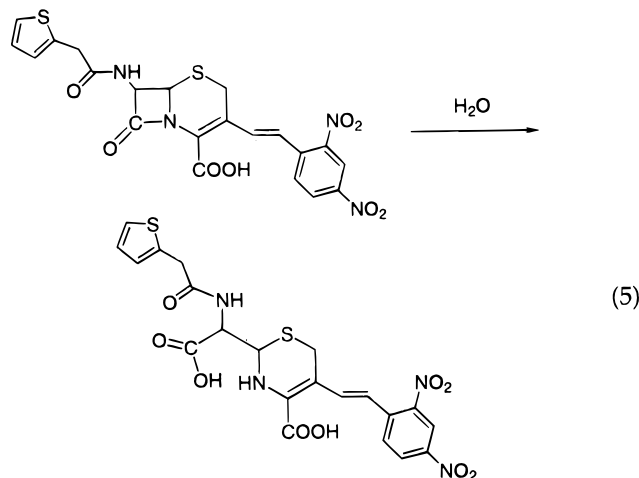
Mechanism for Phosphodiester Hydrolysis. The overall mechanism for hydrolysis of bis(*p*-nitrophenyl)phosphate, (abbreviated $(\text{PhO})_2\text{PO}_2^-$ for convenience, derived from these experiments is summarized in Scheme 5. Displacement of diphen-

Scheme 5



ylphosphinate in $[\text{Zn}_2(\text{BPAN})(\mu\text{-OH})(\mu\text{-O}_2\text{PPh}_2)]^{2+}$ by substrate is followed by external attack of water at the phosphorus atom. This attack is promoted by the bridging hydroxide which serves as a general base. Transesterification of 2-hydroxypropyl-*p*-nitrophenyl phosphate also involves general-base catalysis by the $\mu\text{-OH}$ group in $[\text{Zn}_2(\text{BPAN})(\mu\text{-OH})(\mu\text{-O}_2\text{PPh}_2)]^{2+}$.²⁶

Hydrolysis of Nitrocefim by the Dinuclear Complex. Nitrocefim, a β -lactam substrate (eq 5), undergoes a characteristic



color change when hydrolyzed, and is widely used in assays and kinetic studies of β -lactamases and their model complexes.^{27,43} The absorbance maximum at 390 nm ($\epsilon_{390} = 21\,000 \text{ M}^{-1} \text{ cm}^{-1}$) in nitrocefim shifts to 486 nm ($\epsilon_{486} = 10\,000 \text{ M}^{-1} \text{ cm}^{-1}$) upon hydrolysis due to the formation of the corresponding cephalosporanoic acid, as indicated in eq 5.

The complex $[\text{Zn}_2(\text{BPAN})(\mu\text{-OH})(\mu\text{-O}_2\text{PPh}_2)](\text{ClO}_4)_2$ also promotes the hydrolysis of nitrocefim according to eq 5. Rate enhancements in reactions effected by the dinuclear complex are 2.3 and 2.8×10^3 relative to $\text{Zn}(\text{NO}_3)_2$ and background hydrolyses, respectively (Table 1). Intermediates were not

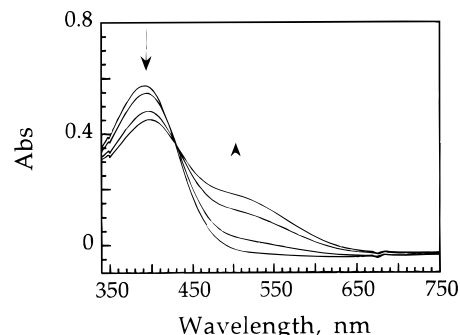


Figure 4. Hydrolysis of nitrocefim in a 1:9 mixture of DMSO and 0.050 M HEPES buffer followed by UV-vis spectrophotometry in the presence of $[\text{Zn}_2(\text{BPAN})(\mu\text{-OH})(\mu\text{-O}_2\text{PPh}_2)](\text{ClO}_4)_2$. The initial concentration of the complex was $5.0 \times 10^{-4} \text{ M}$.

detected when the reaction was carried out in aqueous solution, as the UV-vis spectrophotometric data in Figure 4 reveal.

Binding of β -Lactam Substrates to $[\text{Zn}_2(\text{BPAN})(\mu\text{-OH})(\mu\text{-O}_2\text{PPh}_2)](\text{ClO}_4)_2$. Coordination of β -lactam substrates does not significantly affect their absorbance maxima, extinction coefficients, or ^1H NMR chemical shifts. The carbonyl region of ^{13}C NMR spectra is sensitive to coordination, however.^{44–46} Cephalothin, a nitrocefim analogue, is readily available and in the presence of $[\text{Zn}_2(\text{BPAN})(\mu\text{-OH})(\mu\text{-O}_2\text{PPh}_2)](\text{ClO}_4)_2$ undergoes slow hydrolysis to yield a product similar to hydrolyzed nitrocefim (Supporting Information). Upon addition of $[\text{Zn}_2(\text{BPAN})(\mu\text{-OH})(\mu\text{-O}_2\text{PPh}_2)](\text{ClO}_4)_2$ to a solution of cephalothin (Scheme 2) two out of three carbonyl resonances undergo a chemical shift change. The downfield shift of the carboxylate resonance is indicative of metal ion coordination.⁴⁶ The downfield shift of the β -lactam carbonyl resonance might similarly arise from coordination of oxygen to zinc(II). Infrared data, however, argue against such binding because no significant shift in $\nu_{\text{C=O}}^{\beta\text{-lactam}}$ was observed (see Experimental Section). The ν_{COO} band at 1626 cm^{-1} is consistent with monodentate coordination of the carboxylate group to zinc(II).^{47–49} We therefore conclude that cephalothin coordinates to $[\text{Zn}_2(\text{BPAN})(\mu\text{-OH})(\mu\text{-O}_2\text{PPh}_2)](\text{ClO}_4)_2$ only via its carboxylate group. The downfield shift experienced by the β -lactam carbonyl group appears to be an indirect effect.

Binding of a β -lactam substrate might affect the integrity of the dimetallic complex resulting in complete or partial substitution of either the bridging diphenylphosphinate or hydroxide ligand. ^{31}P NMR spectra of $[\text{Zn}_2(\text{BPAN})(\mu\text{-OH})(\mu\text{-O}_2\text{PPh}_2)](\text{ClO}_4)_2$ in the presence and absence of penicillin G (sodium salt) were studied in the two solvent systems (Figure S1). Upon addition of penicillin G, the ^{31}P NMR resonance of bound Ph_2PO_2^- shifted by 4 and 6 ppm upfield, as the spectra in Figure S1 reveal. Control experiments clearly demonstrate that the new peak corresponds to free Ph_2PO_2^- . Consequently, penicillin G replaces diphenylphosphinate, which is a relatively weak ligand and does not inhibit hydrolysis of β -lactam substrates significantly.

(43) O'Callaghan, C. H.; Morris, A.; Kirby, S. M.; Shingler, A. H. *Antimicrob. Agents Chemother.* **1972**, *1*, 283–288.

(44) Mondelli, R.; Ventura, P. J. *Chem. Soc., Perkin Trans. 2* **1977**, 1749–1752.

(45) Kaminskaia, N. V.; Kostic, N. M. *Inorg. Chem.* **1997**, *36*, 5917–5926.

(46) Woon, T. C.; Wickramasinghe, W. A.; Fairlie, D. P. *Inorg. Chem.* **1993**, *32*, 2190–2194.

(47) Kupka, T. *Spectrochim. Acta, Part A* **1997**, *53*, 2649–2658.

(48) Ferrer, E. G.; Williams, P. A. M. *Polyhedron* **1997**, *19*, 3323–3325.

(49) Zevaco, T. A.; Görls, H.; Dinjus, E. *Polyhedron* **1998**, *17*, 2199–2206.

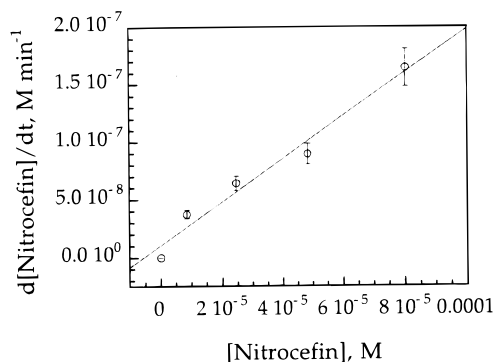


Figure 5. Effect of nitrocefin concentration on the observed rate constant of its hydrolysis promoted by $[\text{Zn}_2(\text{BPAN})(\mu\text{-OH})(\mu\text{-O}_2\text{PPh}_2)](\text{ClO}_4)_2$. Initial concentration of the complex was 5.0×10^{-4} M.

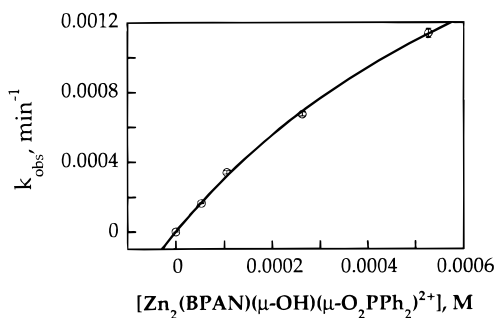


Figure 6. Effect of $[\text{Zn}_2(\text{BPAN})(\mu\text{-OH})(\mu\text{-O}_2\text{PPh}_2)](\text{ClO}_4)_2$ concentration on nitrocefin hydrolysis in aqueous solution. Initial concentration of the substrate was 3.8×10^{-5} M.

Rate Law for the Hydrolysis of Nitrocefin. Hydrolysis promoted by $[\text{Zn}_2(\text{BPAN})(\mu\text{-OH})(\mu\text{-O}_2\text{PPh}_2)](\text{ClO}_4)_2$ depends on the concentration of substrate, as shown in Figure 5. As expected, the hydrolysis rate increases with the concentration of $[\text{Zn}_2(\text{BPAN})(\mu\text{-OH})(\mu\text{-O}_2\text{PPh}_2)](\text{ClO}_4)_2$ (Figure 6), but the dependence is not linear. The saturation kinetics plot in Figure 6 results from substrate coordination to the dizinc complex, according to Scheme 3. Fitting the experimental data in Figure 6 to eq 6 (which was derived for the reaction in Scheme 3)

$$k_{\text{obs}} = \frac{Kk_2[\text{Zn}_2\text{L}]}{K[\text{Zn}_2\text{L}] + 1} \quad (6)$$

yielded binding (K) and microscopic rate (k_2) constants of $(1.1 \pm 0.2) \times 10^3 \text{ M}^{-1}$ and $(3.2 \pm 1.0) \times 10^{-3} \text{ min}^{-1}$, respectively, required in the kinetic analysis. The coordination of nitrocefin to $[\text{Zn}_2(\text{BPAN})(\mu\text{-OH})(\mu\text{-O}_2\text{PPh}_2)](\text{ClO}_4)_2$ is in good accord with the spectroscopic data.

Effect of pH on the Hydrolysis of Nitrocefin. Nitrocefin is hydrolyzed by $[\text{Zn}_2(\text{BPAN})(\mu\text{-OH})(\mu\text{-O}_2\text{PPh}_2)](\text{ClO}_4)_2$ more efficiently at higher pH values, as revealed in Figure 7. The nonlinear dependence is consistent with $\text{Zn}_2\text{-OH}$ acting as the reactive species in hydrolysis. The experimental data were fit to eq 7 which was derived for the mechanism in Scheme 4.

$$k_{\text{obs}} = \frac{k_{\text{H}_2\text{O}}[\text{H}^+] + k_{\text{OH}}K_a}{K_a + [\text{H}^+]} \quad (7)$$

Therefore, $k_{\text{H}_2\text{O}}$ and k_{OH} are rate constants corresponding to hydrolysis of nitrocefin by the aqua and hydroxo complexes. Their respective values are 7.5×10^{-4} and $3.4 \times 10^{-2} \text{ min}^{-1}$. As expected, the hydroxo complex is more reactive than the aqua complex. The fit also afforded the kinetically important $\text{p}K_a$

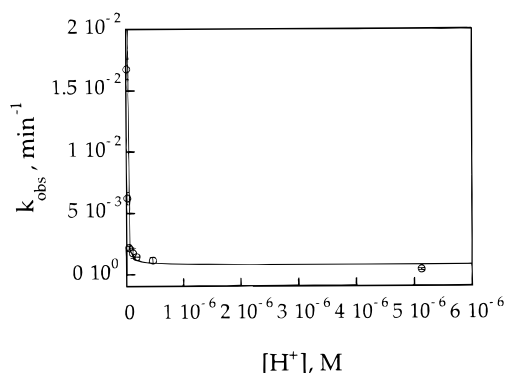


Figure 7. Effect of solution pH on nitrocefin hydrolysis promoted by $[\text{Zn}_2(\text{BPAN})(\mu\text{-OH})(\mu\text{-O}_2\text{PPh}_2)](\text{ClO}_4)_2$. Initial concentrations of the complex and substrate were 5.0×10^{-4} and 3.8×10^{-5} M, respectively.

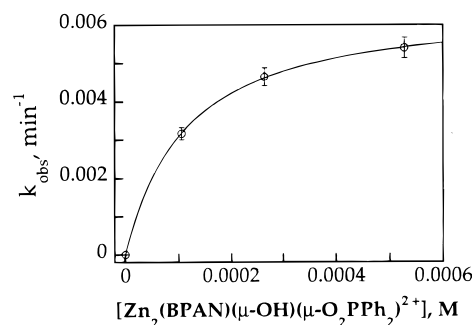


Figure 8. Effect of $[\text{Zn}_2(\text{BPAN})(\mu\text{-OH})(\mu\text{-O}_2\text{PPh}_2)](\text{ClO}_4)_2$ concentration on nitrocefin hydrolysis in organic solvent in the presence of 0.28 M H_2O . Initial concentration of the substrate was 3.8×10^{-5} M.

value of 8.7 ± 0.2 . This value is identical to that obtained from the potentiometric titration experiments for terminal water deprotonation.²⁶ We therefore conclude that in aqueous solution the terminal hydroxide ion in this complex is the reactive species in nitrocefin hydrolysis, whereas the bridging hydroxide is inactive.

Hydrolysis rate constants for nitrocefin at various dizinc(II) complex concentrations in a 1:9 mixture of DMSO and acetone containing 0.28 M H_2O are shown in Figure 8. Fitting the experimental data to eq 6 yielded a binding constant K and the microscopic rate constant k_2 of $(8.9 \pm 0.3) \times 10^3 \text{ M}^{-1}$ and $(6.6 \pm 1.6) \times 10^{-3} \text{ min}^{-1}$, respectively. Nitrocefin binding is weaker in the presence of water, presumably because water competes with β -lactam substrates for coordination to $[\text{Zn}_2(\text{BPAN})(\mu\text{-OH})(\mu\text{-O}_2\text{PPh}_2)](\text{ClO}_4)_2$. Apparently, the water concentration does not significantly affect k_2 . The lack of first-order dependence of the microscopic rate constant k_2 on the concentration of water is diagnostic of intramolecular attack of Zn(II)-bound hydroxide or water at coordinated nitrocefin.

Inhibition of the Nitrocefin Hydrolysis. Succinate and acetate ions are efficient inhibitors of $[\text{Zn}_2(\text{BPAN})(\mu\text{-OH})(\mu\text{-O}_2\text{PPh}_2)](\text{ClO}_4)_2$ as the data in Figure 9 reveal. To fit the data we considered the mechanism drawn in Scheme 6, in which both free and inhibitor-bound complexes are reactive in nitrocefin hydrolysis. Fitting the experimental data in Figure 9A to eq 8 afforded a binding constant for succinate, K_2 , of $3328 \pm$

$$k_{\text{obs}} = \frac{k_{\text{Zn}_2\text{L}} + k_{\text{Zn}_2\text{L-1}}K_2[\text{I}]}{1 + K_2[\text{I}]} \quad (8)$$

900 M^{-1} . The rate constants for the free ($k_{\text{Zn}_2\text{L}}$) and inhibitor-bound complex ($k_{\text{Zn}_2\text{L-1}}$) are 1.74×10^{-3} and $3.5 \times 10^{-4} \text{ min}^{-1}$, respectively. Inhibition by acetate, shown in Figure 9B, was also fit to eq 8. The equilibrium constant K_2 of $670 \pm 160 \text{ M}^{-1}$

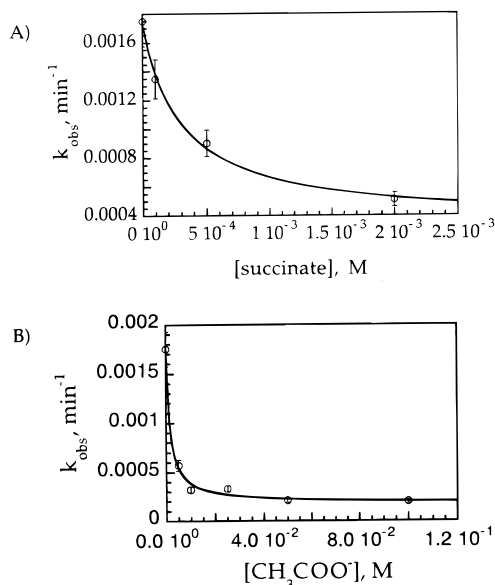
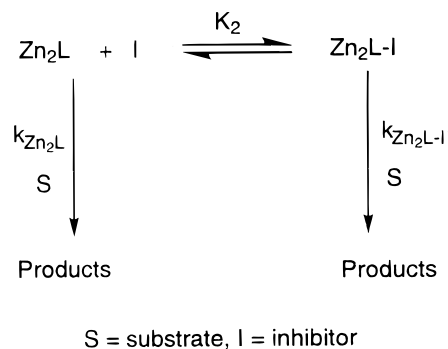


Figure 9. Effect of sodium succinate (A) and sodium acetate (B) concentration on nitrocefin hydrolysis promoted by $[\text{Zn}_2(\text{BPAN})(\mu\text{-OH})(\mu\text{-O}_2\text{PPh}_2)](\text{ClO}_4)_2$. Concentrations of the stock solutions of succinate and acetate were each 0.50 M. Initial concentrations of the complex and substrate were 5.0×10^{-4} and 3.8×10^{-5} M, respectively.

Scheme 6



and the rate constants for the free and inhibitor-bound complex of 1.75×10^{-3} and $1.8 \times 10^{-4} \text{ min}^{-1}$, respectively, were obtained. The value of the binding constant for acetate (K_2) is in a good agreement with that for nitrocefin (K). This similarity is expected because nitrocefin, like acetate, uses only its carboxylate group to coordinate to the dizinc complex. Clearly, succinate ion is a better inhibitor than acetate ion is because the latter is a weaker ligand.

Diphenylphosphinate is not an efficient inhibitor of nitrocefin hydrolysis, as the data in Figure S2 (Supporting Information) reveal. Fitting the data to eq 8 yielded a binding constant for Ph_2PO_2^- of only $100 \pm 24 \text{ M}^{-1}$.

Temperature Dependence of Nitrocefin Hydrolysis. The hydrolysis by $[\text{Zn}_2(\text{BPAN})(\mu\text{-OH})(\mu\text{-O}_2\text{PPh}_2)](\text{ClO}_4)_2$ obeys the Eyring equation and exhibits a linear plot (Figure 10). A fit to the data gave ΔH^\ddagger and ΔS^\ddagger values of $62.7 \pm 3.2 \text{ kJ M}^{-1}$ and $-130 \pm 10 \text{ J M}^{-1} \text{ K}^{-1}$, respectively, in aqueous solution. These values are in relatively good agreement with those for base hydrolysis of penicillin and hydrolysis of penicillin promoted by the mononuclear complex $[\text{Zn}(\text{cyclen})(\text{OH})]^+$.³² Nitrocefin hydrolysis promoted by $[\text{Zn}_2(\text{BPAN})(\mu\text{-OH})(\mu\text{-O}_2\text{PPh}_2)](\text{ClO}_4)_2$ in the absence of water also exhibits a linear behavior (Figure S3, Supporting Information). Fitting the data afforded ΔH^\ddagger and ΔS^\ddagger values of $96.1 \pm 5.2 \text{ kJ M}^{-1}$ and $-22.4 \pm 12 \text{ J M}^{-1} \text{ K}^{-1}$, respectively. The difference between activation parameters for

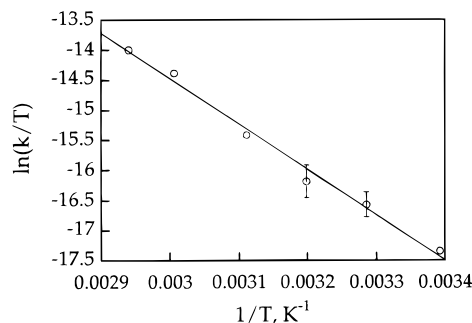


Figure 10. Effect of temperature on nitrocefin hydrolysis promoted by $[\text{Zn}_2(\text{BPAN})(\mu\text{-OH})(\mu\text{-O}_2\text{PPh}_2)](\text{ClO}_4)_2$. Initial concentrations of the complex and substrate were 5.0×10^{-4} and 3.8×10^{-5} M, respectively. The solvent was a 1:9 mixture of DMSO and 0.05 M HEPES buffer.

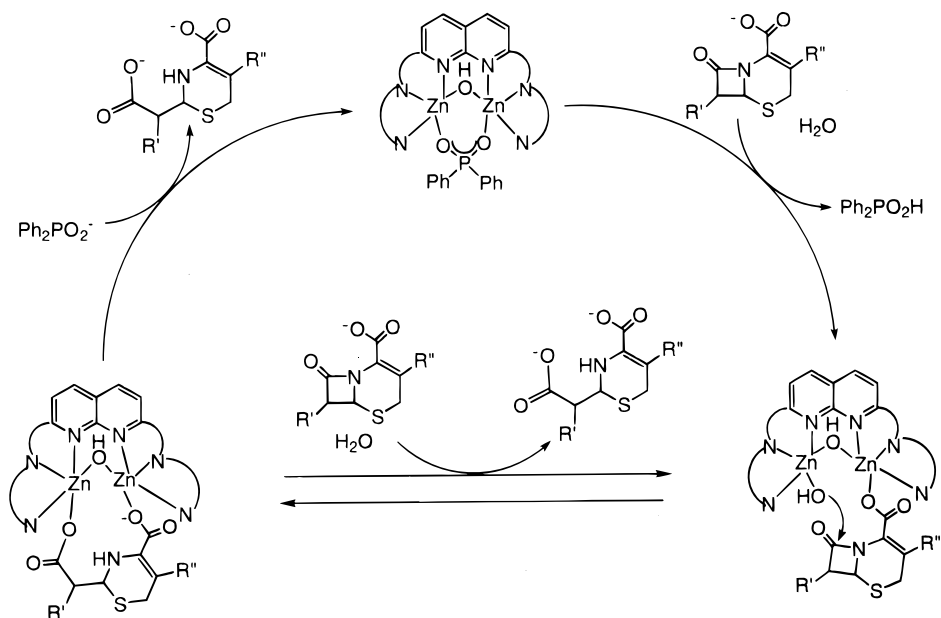
the hydrolysis reaction in aqueous and nonaqueous solutions suggests different reaction mechanisms.

Mechanism for Nitrocefin Hydrolysis. From the foregoing experiments we conclude that nitrocefin hydrolysis by the dinuclear complex in aqueous solution follows the mechanism displayed in Scheme 7. Coordination of the β -lactam carboxylate group to one of the Zn(II) ions is followed by internal nucleophilic attack of the terminally bound hydroxide at the β -lactam carbon atom. The intermediate is rapidly protonated at the β -lactam nitrogen atom and product is released. The complex is a true catalyst because it hydrolyzes more than 8 equiv of nitrocefin, as indicated by the data in Figure S4.

The possibility also exists that the bridging hydroxide ion might shift to a terminal position (Scheme S1) during the course of catalysis. The fact that the complex hydrolyzes nitrocefin in a 1:9 mixture of DMSO and acetone as the solvent seems to agree with such a mechanism in the absence of water (Scheme S1). The respective k_{obs} value of $2.0 \times 10^{-3} \text{ min}^{-1}$ is more than 15-fold lower than that of $3.4 \times 10^{-2} \text{ min}^{-1}$ for the hydrolysis by the terminal hydroxide in Scheme 7. Therefore, hydrolysis occurs even in the absence of the terminal water ligand, albeit slowly. This residual hydrolytic activity presumably results from the $\mu\text{-OH}$ in $[\text{Zn}_2(\text{BPAN})(\mu\text{-OH})(\mu\text{-O}_2\text{PPh}_2)](\text{ClO}_4)_2$. In organic solvents the bridging hydroxide can either attack coordinated substrates directly or shift to a terminal position prior to such attack. Both mechanisms involve two unfavorable processes, attack by a poor nucleophile ($\mu\text{-OH}$) and reorganization of the complex. Hydrolysis is therefore slow. The large activation enthalpy and small activation entropy for the hydrolysis in nonaqueous solution seem to agree with shifting of the bridging hydroxide to a terminal position. The $\text{p}K_{\text{a}}$ value for the shifted hydroxide is expected to be significantly lower than 8.7,³² a kinetically important $\text{p}K_{\text{a}}$. It is therefore unlikely that a hydroxide shift takes place in aqueous solution, where the kinetic $\text{p}K_{\text{a}}$ was determined. These results suggest that hydrolytic mechanisms of $[\text{Zn}_2(\text{BPAN})(\mu\text{-OH})(\mu\text{-O}_2\text{PPh}_2)](\text{ClO}_4)_2$ might differ in the absence and in the presence of water. Similar effects might occur at the active sites of metalloenzymes.

Hydrolyses by Mononuclear Complexes. Mononuclear complexes $\text{Zn}(\text{cyclen})(\text{NO}_3)_2$ and $\text{Zn}(\text{bpta})(\text{OTf})_2$ efficiently hydrolyze both bis(*p*-nitrophenyl)phosphate and nitrocefin, as indicated by the data in Table 1. Their respective $\text{p}K_{\text{a}}$ values of 7.9 and 7.8^{27,32} are sufficiently low that the aqua ligands will deprotonate at physiological pH. The mechanism of phosphodiester hydrolysis involves initial coordination of substrate, followed by intramolecular attack of metal-bound hydroxide at the phosphorus atom.⁵⁰ The relatively high $\text{p}K_{\text{a}}$ value in the mononuclear complex is overcome by the greater reactivity of the terminally bound hydroxide ion. Consequently, $\text{Zn}(\text{bpta})$ -

Scheme 7



(OTf)₂ is only 1.8 times less reactive than [Zn₂(BPAN)(μ -OH)(μ -O₂PPh₂)](ClO₄)₂ in hydrolyzing bis(*p*-nitrophenyl)phosphate.

We investigated the mechanism of Zn(bpta)(NO₃)₂-catalyzed hydrolysis of nitrocefin. As proposed for the mechanism of the dinuclear complex, initial coordination of the substrate is followed by nucleophilic attack of a zinc(II)-bound hydroxide at the β -lactam carbon atom.²⁷ The binding and rate constants were obtained from fitting the data in Figure S5 to eq 6. Their values are $2460 \pm 1000 \text{ M}^{-1}$ and $(7.1 \pm 1.4) \times 10^{-3} \text{ min}^{-1}$, respectively, at pH = 6.95 and 313 K. Considering the similarities between the mechanisms of Zn(bpta)(NO₃)₂ and [Zn₂(BPAN)(μ -OH)(μ -O₂PPh₂)](ClO₄)₂ for nitrocefin hydrolysis, it is not surprising that their reactivities differ very little (Table 1). The hydrolysis catalyzed by Zn(bpta)(NO₃)₂ is twice as rapid as that catalyzed by the dinuclear complex. Solely on the basis of the respective pK_a values of the two complexes, 7.8 and 8.7,^{26,27} Zn(bpta)(NO₃)₂ should be 8 times more reactive than [Zn₂(BPAN)(μ -OH)(μ -O₂PPh₂)](ClO₄)₂. Increased reactivity of the dinuclear complex presumably arises from stabilization of the transition state by the two zinc(II) ions. The dinuclear complex, unlike Zn(bpta)(NO₃)₂, can facilitate nucleophilic attack by interacting with the β -lactam oxygen atom. Although such coordination was not observed for penicillin and cephalothin, it cannot be ruled out for the transition state. The negative value of ΔS^\ddagger supports this conclusion.

Conclusions and Prospects

We have demonstrated that, despite its low pK_a value, the bridging hydroxide in [Zn₂(BPAN)(μ -OH)(μ -O₂PPh₂)](ClO₄)₂ is not very reactive in hydrolytic reactions. Investigations of phosphodiester hydrolysis promoted by the dimetallic complex show that μ -OH acts as a general base, but this apparent advantage does not result in the expected rate enhancements relative to mononuclear complexes. A similar lack of reactivity has been observed in other dizinc(II) model systems.⁵¹

In reactions with the β -lactam substrate nitrocefin, the bridging hydroxide ion is not involved at all, and the terminal

hydroxide acts as the nucleophile. Two possible reasons for this behavior are, first, that the stereochemistry in the [Zn₂(BPAN)(μ -OH)(substrate)]²⁺ complex does not align the μ -OH group properly to attack the coordinated substrate, because they are bound in positions nearly trans to one another.²⁶ Second, the nucleophilicity of the bridging hydroxide is reduced by coordination to two zinc(II) ions. The reaction mechanisms for [Zn₂(BPAN)(μ -OH)(μ -O₂PPh₂)](ClO₄)₂ are therefore better suited to general-base catalysis in the case of bis(*p*-nitrophenyl)phosphate and to the attack by the terminally bound hydroxide in the case of nitrocefin, rather than to nucleophilic attack by the bridging hydroxide ion. Notably, the μ -OH⁻ group serves as a nucleophile in another model system [Zn₂L₁(μ -OH)(NO₃)₂]. The presence of the negatively charged phenoxide ligand and cis-positioning of the coordinated substrate and attacking μ -OH⁻ make nucleophilic attack favorable.²⁷

On the basis of currently available data, it appears that the presence of two zinc ions at the enzymatic active sites is not advantageous for nucleophilic reactivity.⁵² Zinc(II)-bound hydroxide can usually form at mononuclear active sites, albeit at concentrations lower than it can form at dinuclear sites. The lower concentrations, however, are offset by higher reactivity. The possibility that a bridging hydroxide shifts to a terminal position during catalysis in the absence of water cannot be eliminated.⁴

Acknowledgment. This work was supported under the Merck/MIT Collaboration Program. C.H. was the recipient of a Merck/MIT graduate fellowship.

Supporting Information Available: Details of the BPAN synthetic procedures; equations S1 and S2 showing the hydrolyses of phosphate monoesters and bis(*p*-nitrophenyl)phosphate, respectively; Scheme S1 displaying the hydroxide-shift mechanism; and Figures S1–S5 showing ³¹P NMR spectra of [Zn₂(BPAN)(μ -OH)(μ -O₂PPh₂)](ClO₄)₂, inhibition by diphenylphosphinate, temperature dependence in nonaqueous solution, catalytic turnover, and effects of the complex concentration on hydrolysis, respectively. This material is available free of charge via the Internet at <http://pubs.acs.org>.

(50) Young, M. J.; Wahnon, D.; Hynes, R. C.; Chin, J. *J. Am. Chem. Soc.* **1995**, *117*, 9441–9447.

(51) Gultneh, Y.; Allwar; Ahvazi, B.; Blaise, D.; Butcher, R. J.; Jasinski, J.; Jasinski, J. *Inorg. Chim. Acta* **1996**, *241*, 31–38.

IC000169D

(52) Cricco, J. A.; Orellano, E. G.; Rasia, R. M.; Ceccarelli, E. A.; Vila, A. *J. Coord. Chem. Rev.* **1999**, *190–192*, 519–535.